

The First Observation of the *E,Z* Configuration Of Ar–X–N=S=N–X–Ar (X = S, Se) Chains in the Crystalline State

Arkady G. Makarov,^[a] Irina Yu. Bagryanskaya,^[a] Yuri V. Gatilov,^[a] Natalia V. Kuratieva,^[b] Alexander Yu. Makarov,^[a] Makhmut M. Shakirov,^[a] Alexey V. Alexeyev,^[b] Karla Tersago,^[c] Christian Van Alsenoy,^[c] Frank Blockhuys,^{*,[c]} and Andrey V. Zibarev^{*,[a,d]}

Dedicated to Prof. Dr. David W. H. Rankin on the occasion of his retirement

Keywords: Chalcogens / Crystal engineering / Density functional calculations / Configuration determination / Intermolecular interactions / Supramolecular chemistry

New oligomeric analogues of poly(sulfur nitride), i.e. $3\text{-ClC}_6\text{R}_4\text{-X-N=S=N-X-C}_6\text{R}_4\text{Cl-3}$ (**5–8**; R = H, F and X = S, Se), were synthesized and structurally characterized in the solid state by single-crystal XRD, in solution by variable-temperature NMR spectroscopy and in the gas phase with DFT/B3LYP calculations. In the crystal, compounds **5–7** display the well-known *Z,Z* configuration, whereas **8** (R = F, X = Se) is

the first compound to display the *E,Z* configuration amongst twelve structurally defined Ar–X–N=S=N–X–Ar (X = S, Se) derivatives in the hydrocarbon and fluorocarbon series. Through a careful analysis of the packing schemes and the intermolecular interactions of the various compounds, an explanation of the abnormal behaviour of **8** is put forward.

Introduction

Oligomeric analogues of catenated sulfur nitride, $(\text{SN})_x$, a metallic polymer and superconductor,^[1] attract special attention as uncommon π -delocalized polyheteroatom systems, which may find application as molecular wires in the field of molecular electronics.^[2] For this purpose, the understanding of the factors controlling the molecular conformations and, therefore, the molecular π delocalization is of utmost importance. The basic building block in the design and synthesis of oligomeric analogues of $(\text{SN})_x$ is the -N=S=N- unit for which three stereochemical configurations are possible, i.e. the *E,E*, *E,Z* and *Z,Z* configurations. The *E,E* configuration is energetically less favourable^[3] since it leads to the *syn* orientation of the lone pairs of the nitrogen atoms and, therefore, to electrostatic repulsion. In the crystal, the *E,E* configuration is known only for the sterically overcrowded Ar–N=Se=N–Ar deriva-

tive in which Ar = supermesityl.^[4] The stability of the *E,Z* and *Z,Z* configurations is generally comparable, and, for example, for the structurally characterized Ar–N=S=N–Ar derivatives, their occurrence in the solid state is practically the same.^[5]

Elongation of the chalcogen–nitrogen chain leads to interesting structural effects in the solid state. For the two structurally characterized Ar–N=S=N–S–Ar compounds, the *E,Z* configuration was found.^[6] However, for the eight structurally characterized Ar–X–N=S=N–X–Ar (X = S, Se) derivatives bearing Ar groups with various stereoelectronic demands [i.e. both (substituted) hydrocarbon and fluorocarbon groups], only the *Z,Z* configuration was found in the solid state, while the coexistence of the *Z,Z* and *E,Z* isomers was observed by NMR spectroscopy in solution and predicted by quantum chemical calculations in the gas phase.^[7] Ph–N=S=N–S–N=S=N–Ph^[8] and Ph–S–N=S=N–S–N=S=N–S–Ph^[9] possess the *E,Z,E,Z* and *Z,E,Z,Z* configurations in the crystal, respectively, whereas the macromolecular $(\text{SN})_x$ adopts the ...*E,Z,E,Z*... configuration.^[1]

For the Ar–X–N=S=N–X–Ar (X = S, Se) derivatives, it was shown that their configurational preference in the solid state cannot be explained by *intramolecular* stereoelectronic effects, and that *intermolecular* factors (i.e. packing forces) are the main driving force behind the experimentally observed *Z,Z* configurations.^[7] In this situation, the stabilization of the *E,Z* isomer in the crystal can be considered as a challenge for the structural and supramolecular chemistry

[a] Institute of Organic Chemistry, Russian Academy of Sciences, 630090 Novosibirsk, Russia

Fax: +7.383.330.97.52,

E-mail zibarev@nioch.nsc.ru

[b] Institute of Inorganic Chemistry, Russian Academy of Sciences 630090 Novosibirsk, Russia

[c] Department of Chemistry, University of Antwerp, Universiteitsplein 1, B-2610 Wilrijk, Belgium

Fax: +32.3.820.23.10, E-mail frank.blockhuys@ua.ac.be

[d] Department of Physics, Novosibirsk State University, 630090 Novosibirsk, Russia

Supporting information for this article is available on the WWW under <http://dx.doi.org/10.1002/ejic.201000607>.

and crystal engineering of chalcogen–nitrogen compounds. One way to address the problem is by affecting the crystal packing through specific intermolecular interactions,^[10] which are different from the X⋯X interactions observed in the crystal lattices of the already studied *Z,Z* isomers.^[7] Naturally, this way is inherently based on trial-and-error since even the introduction of well-known specific interactions of general applicability^[10] does not automatically lead to the desired control of the supramolecular structure of molecular solids.

The relevant specific intermolecular interactions are, therefore, X⋯Y interactions, where X = S, Se and Y ≠ S, Se, N; even though X⋯N interactions have not been observed in the structures of the already studied derivatives of Ar–X–N=S=N–X–Ar,^[7] nitrogen is included because of the fact that X⋯N interactions do play a very important role in the structural chemistry of a number of other types of chalcogen–nitrogen compounds.^[11] In this situation, Se⋯Cl interactions are probably the most promising. These interactions can be considered as rather strong, since in the case of neutral molecules, they are able to shorten the Se⋯Cl distance to 3.34 Å,^[10] which can directly be compared to the sum of the corresponding van der Waals radii (3.65 Å).^[12] When fluorocarbon derivatives are also considered, the possibility of Cl⋯F interactions^[10] should be taken into account as well.

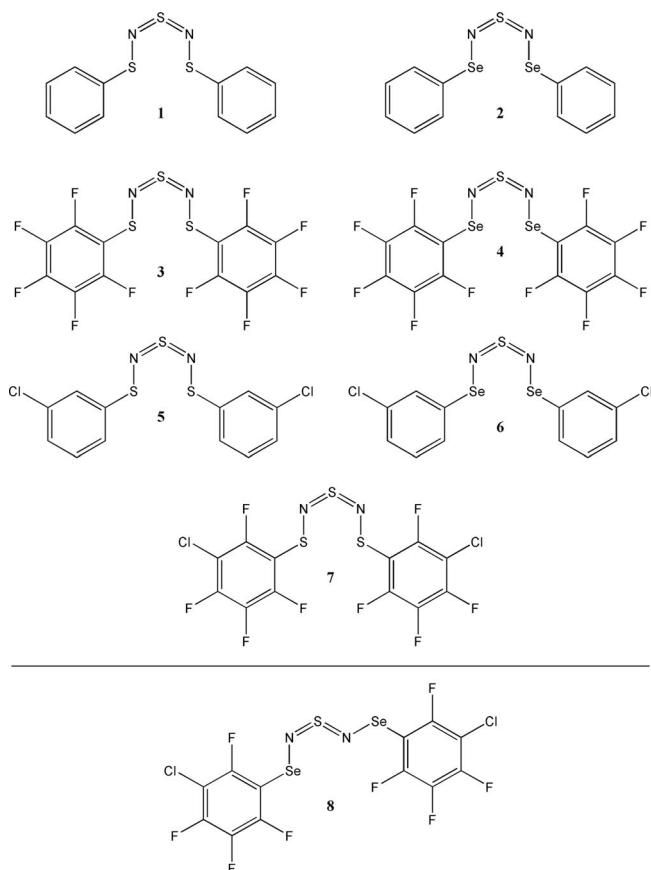
To utilize these Se⋯Cl and Cl⋯F intermolecular interactions, compounds **6** and **8** (Scheme 1) were synthesized. They differ from compounds **2** and **4**, which possess the *Z,Z* configuration in the crystal, only in the presence of two chlorine atoms in the non-resonance *meta* positions; the positioning of these atoms there prevents any major influence on the intramolecular stereoelectronic effects on going from **2** to **6** and from **4** to **8**. At the same time, the presence of these atoms should lead to the desired Se⋯Cl intermolecular interactions in the crystals of both **6** and **8** and also to Cl⋯F interactions in crystals of the latter compound. For comparison, the dithia analogues of **6** and **8**, i.e. compounds **5** and **7** (Scheme 1), were also prepared.

This work reports the preparation of compounds **5–8** and their characterization by single-crystal X-ray diffraction (XRD), variable-temperature NMR spectroscopy and DFT/B3LYP calculations. According to the XRD data, compounds **5–7** display the *Z,Z* configuration typical of all known Ar–X–N=S=N–X–Ar (X = S, Se) derivatives,^[7] while **8** is found to have a *E,Z* configuration. This is the first observation of the *E,Z* configuration in the solid state for these types of compounds.

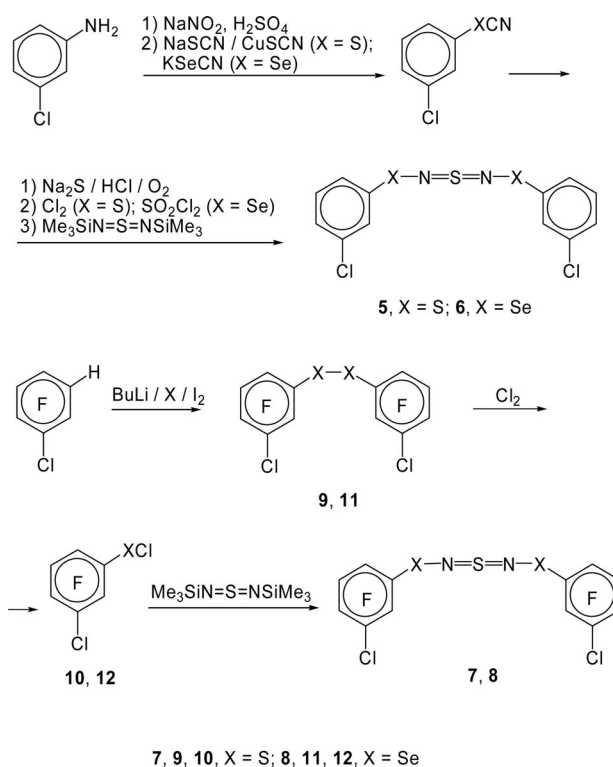
Results and Discussion

Preparation and Solid-State Molecular Structures

Hydrocarbon derivatives **5** and **6** were prepared from 3-chloroaniline, and fluorocarbon derivatives **7** and **8** from 1-chloro-2,3,4,6-tetrafluorobenzene, as represented in Scheme 2.



Scheme 1. Configurations of Ar–X–N=S=N–X–Ar derivatives **1–8** in the crystalline state. For the conformations, see ref. 7 for compounds **1–4** and this work for compounds **5–8**.



Scheme 2. Synthesis of compounds **5–8**.

According to the solid-state structural data given in Table 1, which presents selected bond lengths and bond and torsion angles of compounds **5–8**, derivatives **5–7** possess the *Z,Z* configuration in the crystal, whereas derivative **8** is found in the *E,Z* configuration: Figure 1 depicts the solid-state molecular structures. In the *Z,Z* configurations, the X1...X5 (X = S, Se) distances (Table 1) are shorter than the sum of corresponding van der Waals radii (3.60 Å for S...S and 3.80 Å for Se...Se),^[12] which is typical for this class of compounds: the nature of this shortened contact was discussed before.^[7] The addition of the three new compounds that display the *Z,Z* configuration, i.e. **5**, **6** and **7**, to the eight^[7] already known compounds strengthens the idea that “under normal circumstances” packing forces in the crystal favour this particular configuration.

Table 1. Selected solid-state geometrical data of compounds **5** (X = S), **6** (X = Se), **7** (X = S) and **8** (X = Se); bond lengths in Å and angles in degrees. For the numbering of the atoms, see Figure 1.

	5	6	7	8
C–X1	1.768(4)	1.912(4)	1.760(2)	1.928(10)
X1–N2	1.667(4)	1.845(3)	1.688(2)	1.855(8)
N2–S3	1.554(4)	1.533(4)	1.543(2)	1.514(9)
S3–N4	1.571(4)	1.544(4)	1.544(2)	1.559(9)
N4–X5	1.672(5)	1.856(4)	1.693(2)	1.876(9)
X5–C	1.763(4)	1.919(4)	1.759(2)	1.919(11)
X1...X5	3.252(2)	3.3491(9)	3.2054(9)	4.655(2)
C–X1–N2	101.0(2)	94.4(2)	97.68(9)	95.4(4)
X1–N2–S3	125.9(3)	127.8(2)	127.3(1)	114.1(5)
N2–S3–N4	123.9(2)	126.9(2)	124.3(1)	109.2(5)
S3–N4–X5	126.8(2)	123.7(2)	124.6(1)	112.3(5)
N4–X5–C	99.6(2)	96.2(2)	98.11(9)	95.6(4)
C–X1–N2–S3	–161.4(3)	168.5(3)	–170.3(1)	–174.0(5)
X1–N2–S3–N4	3.6(4)	–4.3(5)	–2.5(2)	0.0(7)
N2–S3–N4–X5	5.9(4)	–0.1(4)	–1.3(2)	175.6(5)
S3–N4–X5–C	–166.5(3)	140.3(3)	–172.4(1)	107.0(6)

In order to verify that the solid-state structure obtained for **8** is representative of the whole sample, its X-ray powder diffraction pattern was recorded. The diffractogram, given in Figure S1 in the Supporting Information, corresponds to that of the single crystal. Therefore, the *E,Z* isomer represents the bulk of the substance.

Gas-Phase Molecular Structures

Since the configuration of interest was indeed experimentally observed for compound **8**, the quantum chemical calculations initially focused on derivatives **7** and **8**. Since the phenyl rings in these compounds do not have axial symmetry (compared to the parent compounds **1** and **2** in which they do), there are more possible structures for each of the conformers. For example, the *Z,Z-anti,anti* conformer of **7** exists both as a C_2 -symmetrical conformer in which the carbon–chlorine bonds are directed away from each other and as a C_1 -symmetrical conformer in which they are located on the same side of the molecule. Both have a different energy, but the difference is small: in this case it is 0.30 kJ mol^{–1} in favour of the C_1 -conformer. For the two other lowest-energy conformers [*E,Z-anti,anti* and

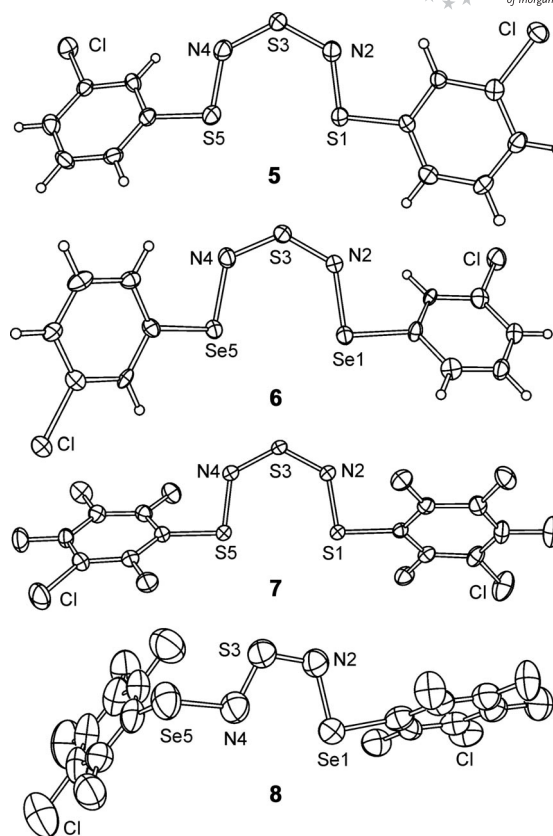


Figure 1. Molecular structures and partial numbering schemes of compounds **5–8**. Displacement ellipsoids are drawn at the 50% probability level; hydrogen atoms are represented by spheres of arbitrary radius.

E,Z-syn,anti], similar considerations can be made (even though the symmetries are C_1 in all cases): for the *E,Z-anti,anti* conformer, the energy difference is 0.31 kJ mol^{–1} in favour of the structure in which the carbon–chlorine bonds are directed away from each other, while for the *E,Z-syn,anti* conformer the difference is 0.25 kJ mol^{–1} in favour of the structure with the two chlorine atoms on the same side of the molecule. In each case, the structure with the lowest energy was used.

The calculated relative energies of the three lowest-energy conformers [*Z,Z-anti,anti*, *E,Z-anti,anti* and *E,Z-syn,anti*] of compounds **7** and **8** have been compiled in Table 2, together with those for compound **4**. We note that all other possible conformers have energies that are considerably higher (>14 kJ mol^{–1}), and as a result, they can be confidently excluded. The data in Table 2 indicate that the *Z,Z-anti,anti* conformer is the lowest-energy conformer for **7** (which is also the conformer that is found in the crystal). In analogy with previous observations,^[7] there are two *E,Z* conformers with an energy low enough such that they will be present in the gas phase (or in solution) at room temperature. On the basis of the results of the calculations, the equilibrium conformer composition at 293 K is 68% *Z,Z-anti,anti*, 28% *E,Z-anti,anti* and 4% *E,Z-syn,anti*. However, for **8**, the *E,Z-anti,anti* conformer (which is also the conformer that is found in the crystal) is the most stable. The

Z,Z-anti,anti and *E,Z-syn,anti* conformers remain in the low-energy set, but the equilibrium conformer composition at 293 K is now 17% *Z,Z-anti,anti*, 77% *E,Z-anti,anti* and 6% *E,Z-syn,anti*.

Table 2. Calculated energies E (in H) and relative energies ΔE (in kJ mol^{-1}) of the three lowest-energy conformers [*Z,Z-anti,anti*, *E,Z-anti,anti* and *E,Z-syn,anti*] for compounds **4**, **7** and **8** at the B3LYP/6-311+G* level of theory. See text for details.

Compound	Conformer	E	ΔE
4	<i>Z,Z-a,a</i>	-6766.7674	4.27
	<i>E,Z-a,a</i>	-6766.7690	0.00
	<i>E,Z-s,a</i>	-6766.7666	6.36
7	<i>Z,Z-a,a</i>	-3480.8139	0.00
	<i>E,Z-a,a</i>	-3480.8131	2.21
	<i>E,Z-s,a</i>	-3480.8112	7.20
8	<i>Z,Z-a,a</i>	-7487.4870	3.68
	<i>E,Z-a,a</i>	-7487.4884	0.00
	<i>E,Z-s,a</i>	-7487.4861	6.17

The molecular geometries of the three conformers are given in Table 3. A comparison of the different calculated stable conformations of the two compounds reveals that when changing the conformation and/or configuration of the molecule, the geometrical changes are quite substantial for the parameters directly involved in the change, i.e. S3–N4, N4–X5 and the three angles in the XNSNX fragment: differences of up to 0.052 Å for N4–S5 in **7** and 16.9° for N2–S3–N4 in **8** are found. These results are analogous to the ones found previously.^[7] By comparing the XRD data of compounds **7** and **8** in Table 1 with those of the relevant gas-phase conformers *Z,Z-anti,anti* for **7** and *E,Z-anti,anti* for **8** in Table 3, it is clear that the qualitative agreement between the calculated and experimental structures is quite good. The differences between single and double bonds are well reproduced, as are the different angles and torsion angles in the heteroatomic fragment. A quantitative comparison indicates that the calculations overestimate the bond lengths, but this is mainly due to the fact that r_{XRD} are r_{a} -type distances, while $r_{\text{calcd.}}$ are r_{c} distances by definition.^[13,14] The deviations are larger for the nonbonded Se...Se and S...S distances, but since these are more sensitive to the crystal environment than the bonded ones, this is to be expected.

The energy values compiled in Table 2 then lead to the following. The values of the relative energy of the *E,Z-anti,anti* isomer of compounds **2**,^[7] **4** and **8**, relative to the *Z,Z-anti,anti* isomer, are +0.38, -4.27 and -3.68 kJ mol^{-1} , respectively. Apparently, the introduction of the fluorine atoms (**2** → **4**) shifts the equilibrium toward the *E,Z* isomer, while the replacement of the fluorine atoms in the 3-positions of the rings with chlorine atoms (**4** → **8**) shifts it back a bit toward the *Z,Z* isomer, even though the difference between the latter two values is rather small. Similar conclusions can be drawn from the values calculated for the sulfur analogues **1**,^[7] **3**^[7] and **7**, which are +5.18, +2.65 and +2.21 kJ mol^{-1} : even though for these systems the shift in the equilibrium toward the *E,Z* isomers continues throughout the series, the difference between the latter two values

Table 3. Selected calculated geometrical data of the three lowest-energy conformers of compounds **7** (X = S) and **8** (X = Se); bond lengths in Å and angles in degrees. For the numbering of the atoms, see Figure 1.

	7			8		
	<i>Z,Z-a,a</i>	<i>E,Z-a,a</i>	<i>E,Z-s,a</i>	<i>Z,Z-a,a</i>	<i>E,Z-a,a</i>	<i>E,Z-s,a</i>
C–X1	1.781	1.783	1.781	1.931	1.932	1.930
X1–N2	1.709	1.706	1.712	1.869	1.865	1.869
N2–S3	1.569	1.564	1.570	1.565	1.561	1.567
S3–N4	1.568	1.600	1.580	1.564	1.598	1.580
N4–X5	1.707	1.744	1.692	1.867	1.899	1.857
X5–C	1.781	1.779	1.795	1.932	1.930	1.942
X1...X2	3.428	4.670	4.616	3.460	4.804	4.783
C–X1–N2	98.1	96.8	96.7	94.5	93.1	93.2
X1–N2–S3	128.2	119.6	119.4	127.3	116.9	117.3
N2–S3–N4	125.0	109.3	110.7	125.7	108.8	110.5
S3–N2–X5	128.6	113.9	127.0	127.8	113.7	125.0
N4–X5–C	98.0	99.2	107.6	94.3	97.2	105.0
C–X1–N2–S3	153.3	177.7	-179.8	147.0	178.4	178.9
X1–N2–S3–N4	-1.0	-0.8	-0.1	-0.8	0.1	0.3
N2–S3–N4–X1	-1.3	-172.9	178.8	-1.0	-173.2	179.8
S3–N4–X1–C	156.9	-121.5	-1.0	150.7	-112.0	-2.5

is also small. In any case, for compounds **1**, **3** and **7**, the *Z,Z* isomer remains the most stable.

An analysis of the intramolecular effects, which may lie at the basis of the influence of the fluorine and/or chlorine atoms on the position of the isomeric equilibrium, may be based on two molecular properties relevant to the bonding in the chalcogen–nitrogen fragments: Tables 4 and 5 present Hirshfeld bond orders^[15] and values of the electron density in bond (BCP) and ring critical points (RCP) according to the quantum theory of atoms in molecules (QTAIM),^[16] respectively, for a selected number of bonds in compounds **4**, **7** and **8**. The data in Tables 4 and 5 can directly be compared to those of the parent systems, **1** and **2** and the derivatives previously studied,^[7] and display exactly the same trends as for those earlier compounds. For **4**, the values increase slightly when going from the *anti,anti* conformers to the *syn,anti* conformer, but this is not seen for **8**. At this time, there are no indications of the factors associated with the presence or absence of either the fluorine atoms or the chlorine atoms in the 3-positions of the aromatic rings, which are responsible for the extra stabilization of the *E,Z* configuration. Further investigations based on calculated atomic and bond properties and a more detailed topological analysis of the electron density and its derivatives are needed and will be performed in the near future.

Nevertheless, all but one compound mentioned in the previous paragraphs are found in the *Z,Z* configuration in the solid state, even compound **4** for which the largest stabilization of the *E,Z* isomer in the gas phase was calculated. Again, this illustrates the particular stabilization of the *Z,Z* isomer in the crystal environment, described earlier. At this moment, compound **8** is the only compound for which the *E,Z* isomer is found both in the gas phase and in the crystal. Before we continue with an analysis of the crystal packing and the intermolecular contacts in an attempt to clarify the unusual behaviour of compound **8**, the results of a

Table 4. Hirshfeld bond orders for the three lowest-energy conformers of compounds **4** (X = Se), **7** (X = S) and **8** (X = Se). See text for details.

	4			7			8		
	Z,Z- <i>a,a</i>	E,Z- <i>a,a</i>	E,Z- <i>s,a</i>	Z,Z- <i>a,a</i>	E,Z- <i>a,a</i>	E,Z- <i>s,a</i>	Z,Z- <i>a,a</i>	E,Z- <i>a,a</i>	E,Z- <i>s,a</i>
C–X1	0.94	0.93	0.94	1.09	1.08	1.08	0.94	0.93	0.94
X1–N2	1.00	0.97	0.97	1.19	1.17	1.15	0.99	0.97	0.97
N2–S3	1.86	1.82	1.81	1.83	1.80	1.79	1.86	1.82	1.81
S3–N4	1.86	1.61	1.70	1.84	1.59	1.69	1.87	1.61	1.70
N4–X5	1.00	0.91	1.07	1.20	1.07	1.30	1.00	0.90	1.07
X5–C	0.94	0.96	0.93	1.09	1.11	1.06	0.94	0.96	0.93
X1⋯X5	–0.41	–0.68	–0.68	–0.51	–0.68	–0.68	–0.41	–0.68	–0.68

Table 5. Values of the electron density $\rho(r)$ (in a.u.) of the relevant BCPs and RCPs for the three lowest-energy conformers of compounds **4** (X = Se), **7** (X = S) and **8** (X = Se). See text for details.

		4			7			8		
		Z,Z- <i>a,a</i>	E,Z- <i>a,a</i>	E,Z- <i>s,a</i>	Z,Z- <i>a,a</i>	E,Z- <i>a,a</i>	E,Z- <i>s,a</i>	Z,Z- <i>a,a</i>	E,Z- <i>a,a</i>	E,Z- <i>s,a</i>
BCP	C–X	0.1472	0.1475	0.1882	0.1911	0.1910	0.1911	0.1473	0.1480	0.1480
	X1⋯X5	0.0113	–	–	0.0086	–	–	0.0113	–	–
RCP	C ₆ R ₅	0.0201	0.0195	0.0486	0.0196	0.0201	0.0221	0.0201	0.0210	0.0198
	NSNX⋯X	0.0082	–	–	0.0074	–	–	0.0083	–	–

number of NMR spectroscopic measurements, consistent with the results of the calculations, are presented.

Variable-Temperature NMR Spectroscopy

Multinuclear NMR spectroscopic data for compounds **5–8**, measured at 303 K in chloroform, are presented in Table 6. ⁷⁷Se and ¹⁹F NMR spectroscopy allow the verification of the presence of more than one isomer in solutions of the derivatives by virtue of variable-temperature measurements.

Previous variable-temperature ⁷⁷Se NMR measurements on **2** (which possesses the Z,Z configuration in the crystal) resulted in the conclusion that, in toluene at 203 K, compound **2** exists as a (roughly) 1:1 equilibrium mixture of the Z,Z and E,Z isomers.^[7] This solution behaviour is typical of catenated chalcogen–nitrogen compounds.^[5,17] On the basis of this conclusion, as well as on the results of the aforementioned DFT/B3LYP calculations, we assumed that more than one isomer should be visible in the ⁷⁷Se and ¹⁹F NMR spectra of **6** and **8** and in the ¹⁹F NMR spectra of **7**, keeping in mind that, when extrapolating gas-phase calculated data to a solvent environment, solvent effects cannot be ruled out and one must be very careful when transferring the calculated energy differences to a different aggregation state.

In functionalized aromatic derivatives, the substitution of hydrogen atoms by fluorine atoms normally leads to a high-field shift of the NMR signals of the heavy nuclei positioned α with respect to the aromatic ring: compare, for example, $\delta^{77}\text{Se}$ of C₆H₅SeSeC₆H₅ at $\delta = 460$ ppm with that of C₆F₅SeSeC₆F₅ at $\delta = 368$ ppm.^[18] In toluene, compound **4** (which displays the Z,Z configuration in the crystal)^[7] displays a broad peak in the 303 K ⁷⁷Se NMR spectrum at $\delta = 775$ ppm, which can directly be compared to the corresponding signal at $\delta = 933$ ppm for compound **2** at 323 K.^[7]

Table 6. Multinuclear NMR (measured at 303 K) and UV/Vis data for compounds **5–8** in chloroform: chemical shifts, δ , in ppm and λ_{max} in nm.

	¹ H	¹³ C	NMR			λ_{max} (log ϵ)
			¹⁹ F	¹⁴ N	⁷⁷ Se	
5	7.43,	140.4,	–	–	218 (4.40),	
	7.31,	135.3,			261 (4.15),	
	7.25,	130.1,			447 (4.13)	
	7.20	127.1,				
6	7.57,	136.0,	–	292	[a]	212 (4.63),
	7.42,	135.3,				260 (4.24),
	7.31,	130.3,				412 (3.99)
	7.26	128.5,				
		128.3,				
7	–	128.1,	52.5,	285	–	223 (4.31),
		153.4,	35.8,			361 (3.78),
		150.2,	35.6,			403 (3.76;
		148.8,	2.5			shoulder)
		137.8,				
8	–	110.7,	58.2,	300	793	229 (4.34),
		108.1,	41.6,			370 (3.81),
		153.3,	35.1,			416 (3.50;
		150.2,	2.7			shoulder)
		148.9,				
		137.6,				
	107.8,					
	106.4					

[a] For **6**, the ⁷⁷Se signal at 303 K was too broad to be measured; experiments at a lower temperature were unsuccessful because of the low solubility of the compound.

In contrast to what was found in the crystal, at lower temperatures only the E,Z isomer of **4** was detected with ⁷⁷Se NMR spectroscopy performed in toluene (see Supporting Information, Figure S2), whereas in chloroform an equilibrium of the major E,Z ($\delta^{77}\text{Se}$ 893 and 670; 85%) and the minor Z,Z ($\delta^{77}\text{Se}$ 758; 15%) isomers was observed (Figure S2). With ¹⁹F NMR spectroscopy, only the E,Z config-

uration was observed for **4** in both toluene and chloroform (Figure S3).

The behaviour of compound **8** in solution is very similar to that of **4**. According to the data obtained from variable-temperature ^{19}F and ^{77}Se NMR spectroscopy, in toluene, compound **8** exists exclusively as the *E,Z* isomer, whereas in chloroform solution at 223 K, the compound is found as an equilibrium mixture of the major *E,Z* ($\delta^{77}\text{Se}$ 892 and 669; 90%) and the minor *Z,Z* ($\delta^{77}\text{Se}$ 758; 10%) isomers (Figures S4 and S5).

Calculated ^{77}Se NMR chemical shifts of the three lowest-energy conformers of compound **8** (Table 7) are in reasonable agreement with the low-temperature experimental data for the *E,Z* and *Z,Z* configurations in chloroform. In particular, they correctly place the signal of the *Z,Z-anti,anti* conformer between those of the *E,Z-anti,anti* conformer.

Table 7. Calculated ^{77}Se NMR chemical shifts [in ppm vs. $(\text{CH}_3)_2\text{Se}$] of the three lowest-energy conformers of compound **8**.

	<i>Z,Z-a,a</i>	<i>E,Z-a,a</i>	<i>E,Z-s,a</i>
Se1	806	996	928
Se5	825	731	854

Variable-temperature ^{19}F NMR spectra of **7** in toluene and chloroform reveal dynamics that can be associated with an equilibrium mixture of two isomers consisting of ca. 70% of the major (tentatively *E,Z*) and 30% of the minor (tentatively *Z,Z*) component at 203 K in toluene (compare Figure S6a with S6b and S6c).

For compounds **5** and **6**, the lower-temperature ^1H NMR measurements were limited to ca. 250 K, because of their lower solubility in both toluene and chloroform (compared to the polyfluorinated derivatives **7** and **8**): these measurements did not yield any definitive information on the isomeric equilibria in solutions.

The solution behaviour of the selenium-containing derivatives **2**, **4** and **8** can be summed up by saying that, while there appears to be a ca. 1:1 equilibrium of the *Z,Z* and *E,Z* isomers in the case of **2**, the *E,Z* isomer dominates in the case of its polyfluorinated congeners **4** and **8**. Nevertheless, compound **4** crystallizes in the *Z,Z* configuration,^[7] whereas **8** is found in the *E,Z* configuration. Previously, it was shown by using OPiX simulations that the organization of the *Z,Z* configuration in the crystal has a systematic preference over the organization of the *E,Z* configuration, in both energy and density.^[7] Therefore, a careful analysis of the supramolecular packing and intermolecular interactions of **8** is necessary to determine the factors that stabilize the *E,Z* configuration in this case.

Crystal Packing

The OPiX simulations of the crystal packing^[19] previously used for compound **1** could not be employed in the present study because of the absence of parameters for selenium atoms. The crystal packing schemes of compounds **4–8** are presented in Figure S7 in the Supporting Information (the intermolecular contacts that are shorter than the sum

of the van der Waals' radii by more than 0.1 Å are indicated by dashed lines), but the reader is referred to the CIFs of these compounds for the complete structures. In the supramolecular structures of **4–7**, layers and stacks can be identified. For **4** (Figure S7a), only two F...F contacts of 2.83 and 2.86 Å can be observed in the supramolecular structure. For both **5** and **6**, stacks are formed by $\pi\cdots\pi$ interactions, which feature distances of 3.85 and 3.96 Å between the ring centroids and of 3.48 and 3.47 Å for the interplanar separations, respectively. However, the lateral interactions between these π stacks are different for the two compounds. For **5** (Figure S7b), they are Cl1...Cl2 contacts of 3.40 Å (shorter than the sum of the van der Waals radii by 0.10 Å), whereas the packing of **6** (Figure S7c) displays two CH...N contacts: CH...N1 2.55 Å, 155° and CH...N2 2.56 Å, 176°. In contrast to expectations, the intermolecular Se...Cl contacts in **6** (not represented in Figure S7) are relatively long, as they are a mere 0.09 Å shorter than the sum of van der Waals radii. For **7** (Figure S7d), there are no π -stacking interactions, and layers are formed from laddertype stacks by means of S5...N2 (3.15 Å) and F1...F8 (2.79 Å) contacts – both are 0.20 Å shorter than the sum of the van der Waals radii. An additional CF...Cg (3.07 Å, 127.5°) contact can also be observed (Cg denotes the centroid of a ring). Short S...Cl contacts are not present.

The crystal packing of **8** (Figure S7e) is very different from those of **4–7** and the other studied Ar–X–N=S=N–X–Ar derivatives.^[7] In particular, layers and stacks cannot be observed. In fact, the supramolecular organization of **8** is strongly perturbed, relative to the packing of the other relevant compounds. Analysis of the crystal packing of **8** with respect to intermolecular contacts, which are shorter than the sum of the corresponding van der Waals radii by more than 0.1 Å, reveals Se1...Cl1 contacts of 3.37 Å (the sum of the van der Waals radii is 3.65 Å)^[12,20] and Cl...F contacts of 3.02 and 3.06 Å (the sum of the van der Waals radii is 3.22 Å).^[12,20] Every Cl1 atom participates in two short contacts and every Se1 atom in one, as can be seen in Figure 2 which compares the short intermolecular contacts in **7** and **8**. Analysis of the Cambridge Structural Database reveals that Se...Cl intermolecular interactions are rather widespread, as 62 structures of molecular and ionic compounds with intermolecular Se...Cl distances shorter than the sum of the van der Waals radii were found; therefore, the Se...Cl contact distances observed in **8** can be considered as typical.^[21]

An analysis of the short intermolecular contacts for the whole series of known Ar–X–N=S=N–X–Ar (X = S, Se) derivatives, based on the difference Δ between the observed contact distance and the sum of the relevant van der Waals' radii, leads to the following situation. For the parent compounds **1** and **2**, Δ is only –0.03 for the S...S distances and –0.04 Å for the Se...S distances, respectively. Introduction of chlorine atoms in **5** and **6** and the 4,4'-dichloro derivative of **1**^[7] results in an increase in Δ to –0.10 for Cl...Cl in **5**, –0.20 for N...H and –0.09 for Se...Cl in **6** and –0.21 Å for Cl...Cl in the 4,4'-dichloro derivative of **1**. In the case of polyfluorination in **3** and its 4,4'-bis(trifluoromethyl) deriv-

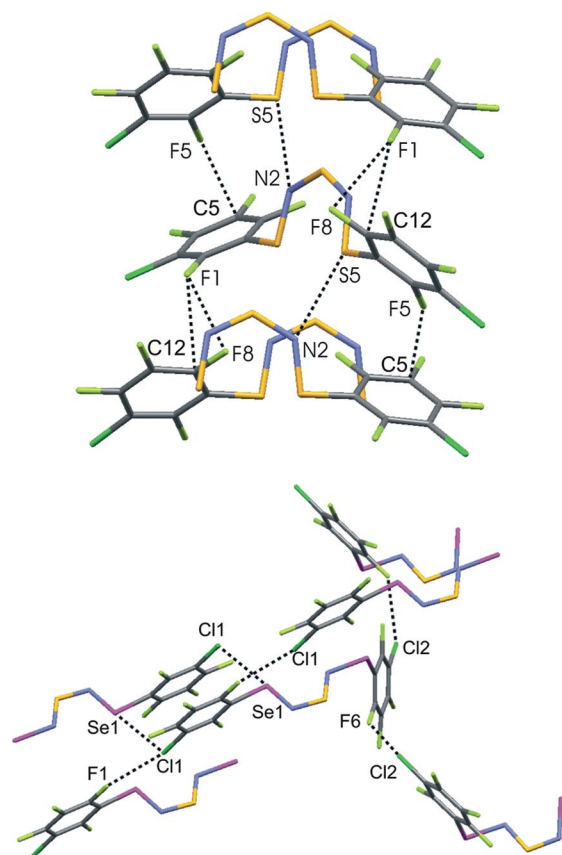


Figure 2. Comparison of the short intermolecular contacts (in Å) in the supramolecular structures of (a) **7** [N2⋯S5 3.15 (−0.20), F1⋯C12 2.99 (−0.18), F5⋯C5 2.99 (−0.18), F1⋯F8 2.79 (−0.15)] and (b) **8** [Cl1⋯Se1 3.37 (−0.28), Cl1⋯F1 3.02 (−0.20), Cl2⋯F6 3.06 (−0.16)] (values in parentheses are the differences between the observed contact distance and the sum of the relevant van der Waals' radii). Note that for clarity a number of phenyl rings have been removed from the peripheral molecules.

ative, **4**, **7** and **8**, the number of short contacts increases, as do their Δ values to -0.19 for F⋯C in **3**, -0.23 for F⋯F in the 4,4'-bis(trifluoromethyl) derivative of **3**, -0.11 for F⋯F in **4**, -0.20 for S⋯N in **7** and -0.28 Å for Se⋯Cl in **8**. On the basis of this and the values presented above for compound **8**, it is clear that the targeted specific intermolecular Se⋯Cl and Cl⋯F interactions were indeed obtained in the supramolecular structure of **8**, obviously leading to the *E,Z* molecular configuration. Furthermore, from the values of the contact distances in **8**, it may be concluded that they belong to the shortest found to date in the solid-state structures of the whole Ar–X–N=S=N–X–Ar series.

Conclusions

It has been shown experimentally that by combining specific Se⋯Cl and Cl⋯F intermolecular interactions it is possible to stabilize the unusual *E,Z* molecular configuration of the Ar–X–N=S=N–X–Ar (X = S, Se) derivatives, oligomeric analogues of polymeric sulfur nitride, (SN)_x, in the crystalline state, against the presence of the *Z,Z* configura-

tion observed in all other cases. This finding is of considerable importance in the structural and supramolecular chemistry and crystal engineering of chalcogen–nitrogen compounds.

Experimental

General

¹H (500.13 MHz), ¹³C (125.8 MHz), ¹⁴N (36.1 MHz) and ⁷⁷Se (95.4 MHz) NMR spectra were measured on a Bruker DRX-500 spectrometer, and ¹⁹F NMR spectra (282.4 MHz) on a Bruker AV-300 spectrometer, for solutions in CDCl₃ at 303 K unless otherwise indicated; standards were TMS (twice), NH₃ (liq.), Me₂Se and C₆F₆ ($\delta^{19}\text{F} = -162.2$ with respect to CFC₃), respectively. High-resolution mass spectra (EI, 70 eV) were measured on a DFS Thermo Electron Corporation instrument. UV/Vis spectra were recorded on a Hewlett–Packard 8453 spectrophotometer for solutions in heptane. GC–MS measurements were performed with a Hewlett–Packard G1800A GCD device for solutions in CH₂Cl₂. The starting materials (Me₃SiN=)₂S,^[22] 3-ClC₆H₄XCN (X = S, Se)^[23] and 1-chloro-2,3,4,6-tetrafluorobenzene^[24] were prepared by known methods. All solvents were distilled under argon with common drying agents. The syntheses described below were carried out at ambient temperature unless otherwise indicated, with stirring. The reagents were added dropwise, and the solvents were distilled off under reduced pressure. In the syntheses of compounds **7** and **8**, a modification of the previously described approach^[25] was used.

Syntheses

1,5-Bis(3-chlorophenyl)-2,4-diaza-1,3,5-trithia-2,3-pentadiene (5): A solution of concentrated HCl (1.6 mL) in H₂O (10 mL) was added to solution of 3-ClC₆H₄SCN (1.16 g, 7 mmol) in Na₂S (6 mL of a 2.33 M aqueous solution). A stream of air was passed through the reaction mixture for 2.5 h, and the mixture was extracted with Et₂O (3 × 20 mL). The extract was dried with MgSO₄, and the solvents evaporated. The residual yellow oil, which contained (GC–MS) 86% of ArSH and 14% of ArSSAr (Ar = 3-ClC₆H₄), was dissolved in CCl₄ (30 mL), and an excess of Cl₂ was passed through the solution at 0 °C. The solvent was distilled off, the residual red oil was dissolved in hexane (30 mL) and added, over a period of 1 h, to a solution of (Me₃SiN=)₂S (0.72 g, 3.5 mmol) in hexane (30 mL), under argon. The solvent was distilled off, and compound **5** (Tables 6 and 8) was obtained as red crystals. Single crystals suitable for XRD were prepared by crystallization from toluene.

1,5-Bis(3-chlorophenyl)-2,4-diaza-1,5-diselena-3-thia-2,3-pentadiene (6): A solution of 3-ClC₆H₄SeCN (1.50 g, 7 mmol) in Na₂S (6 mL of a 2.33 M aqueous solution) was treated with HCl and air as described above. The obtained orange–yellow oil contained (GC–MS) 95% of ArSeSeAr and 5% of AsSeAr (Ar = 3-ClC₆H₄). This oil (1.0 g, ca. 2.6 mmol) was dissolved in CCl₄ (5 mL), and a solution of SO₂Cl₂ (0.2 mL, 2.6 mmol) in CCl₄ (20 mL) was added over a period of 30 min. The solvent was distilled off, the residual dark-red oil was dissolved in hexane (30 mL) and added to a solution of (Me₃SiN=)₂S (0.55 g, 2.6 mmol) in hexane (30 mL) over a period of 1 h and under argon. The solvent was distilled off, and the residue was recrystallized from hexane. Compound **6** (Tables 6 and 8) was obtained as orange–yellow crystals.

1,5-Bis(3-chloro-2,4,5,6-tetrafluorophenyl)-2,4-diaza-1,3,5-trithia-2,3-pentadiene (7): (a) Under argon and at -60 °C, 48 mL of a 0.52 M hexane solution of BuLi (25 mmol) was added, over a period of 30 min, to a solution of 1-chloro-2,3,4,6-tetrafluorobenzene

Table 8. Physical data of compounds: yield (in %), melting point (in °C) or boiling point (in °C/Torr), mass spectroscopic data and elemental composition (in %).

	Yield	m.p. or b.p.	MS (M ⁺ , m/z) ^[a]		Elemental analysis: found (calculated) ^[b]			
			found	calculated	C	H or F	Cl	N
5	64	92–93	345.9236	345.9227	41.22 (41.50)	2.23 (2.32)	20.46 (20.42)	8.04 (8.07)
6	26	80–81	441.8129	441.8116	33.26 (32.68)	2.34 (1.83)	16.15 (16.07)	6.02 (6.35)
7	68	50–51	489.8460	489.8467	29.77 (29.34)	30.87 (30.94)	13.90 (14.43)	6.02 (5.70)
8	36	81–82	585.7377	585.7366	24.67 (24.64)	25.99 (25.98)	12.01 (12.12)	4.42 (4.79)
9	41	<20	429.8687	429.8685	–	–	–	–
10	78	65/3	–	–	–	30.36 (30.27)	–	–
11	58	72–73	525.7567	525.7579	27.53 (27.46)	29.27 (28.95)	13.48 (13.51)	–
12	69	89/3	–	–	24.24 (24.19)	–	–	–

[a] For ³⁵Cl and ⁸⁰Se. [b] For S, found (calculated): for **5**, 27.65 (27.70); for **7**, 19.60 (19.58).

(4.62 g, 25 mmol) in Et₂O (60 mL). After 60 min at the same temperature, finely ground sulfur (0.80 g, 25 mmol) was added. After an additional 75 min, the reaction mixture was warmed up to 0 °C and iodine (3.30 g, 13 mmol) was added, followed by a solution of Na₂S₂O₃·5H₂O (3 g) in H₂O (30 mL). The reaction mixture was extracted with Et₂O (4 × 15 mL), the extract was dried with MgSO₄, and the solvents evaporated. The residue was recrystallized from hexane at –40 °C. 3,3'-Dichloro-2,2',4,4',5,5',6,6'-octafluorodiphenyl disulfide (**9**, Table 8) was obtained as pale-yellow crystals. ¹⁹F NMR: δ = 52.8, 36.0, 35.3, 2.6 ppm. (b) An excess of Cl₂ was passed through a solution of **9** (1.29 g, 3 mmol) in CCl₄ (10 mL). The solvent was distilled off, and the residue was distilled at reduced pressure. 3-Chloro-2,4,5,6-tetrafluorophenylsulfenyl chloride (**10**, Table 8) was obtained as a dark-red oil. ¹⁹F NMR: δ = 56.8, 39.8, 38.7, 2.9 ppm. (c) Under argon, a solution of **10** (0.33 g, 1.3 mmol) in hexane (20 mL) was added, over a period of 1 h, to a solution of (Me₃SiN=)S (0.14 g, 0.66 mmol) in hexane (14 mL). The volume of the reaction mixture was reduced to 2 mL and brought down to –20 °C. Compound **7** (Tables 6 and 8) was obtained as orange–yellow crystals.

1,5-Bis(3-chloro-2,4,5,6-tetrafluorophenyl)-2,4-diaza-1,5-diselena-3-thia-2,3-pentadiene (8): (a) Under argon and at –60 °C, 17.3 mL of a 2.5 M hexane solution of BuLi (43 mmol) was added, over a period of 15 min, to a solution of 1-chloro-2,3,4,6-tetrafluorobenzene (7.97 g, 43 mmol) in Et₂O (100 mL). After an additional 60 min at the same temperature, finely ground selenium (3.41 g, 43 mmol) was added. The reaction mixture was kept at –60 °C for 60 min, warmed up to 0 °C and iodine (5.59 g, 22 mmol) was added. After 30 min at ambient temperature, the reaction mixture was treated with a solution of Na₂S₂O₃·5H₂O (3 g) in H₂O (30 mL) and extracted with Et₂O (4 × 15 mL). The extract was dried with MgSO₄ and evaporated, and the residue was recrystallized from hexane. 3,3'-Dichloro-2,2',4,4',5,5',6,6'-octafluorodiphenyl diselenide (**11**, Table 8) was obtained as yellow crystals. NMR: δ¹³C = 154.4, 150.0, 149.7, 137.3, 107.4, 103.0 ppm; δ¹⁹F = 58.9, 42.2, 34.3, 2.5 ppm; δ⁷⁷Se = 376 ppm. (b) An excess of Cl₂ was passed through a solution of **11** (5.0 g, 10 mmol) in CCl₄ (15 mL). The solvent was distilled off, and the residue was distilled at reduced pressure. 3-Chloro-2,4,5,6-tetrafluorophenylselenenyl chloride (**12**, Table 8) was obtained as a dark-red oil. NMR: δ¹³C = 154.2, 151.3, 149.7, 137.5, 107.8, 104.5 ppm; δ¹⁹F = 62.0, 45.2, 38.0, 3.2 ppm; δ⁷⁷Se = 808 ppm. (c) Under argon and at –30 °C, a solution of **12** (0.45 g, 1.5 mmol) in hexane (30 mL) was added, over a period of 70 min, to a solution of (Me₃SiN=)S (0.15 g, 0.75 mmol) in hexane (10 mL). The reaction mixture was warmed up to 20 °C, and the solvent was distilled off. The residue was recrystallized from hexane at –20 °C. Compound **8** (Tables 6 and 8) was obtained as orange–yellow crystals.

Crystallographic Analysis

Crystallographic data on the four new compounds **5–8** can be found in Table 9. The XRD data were obtained on a Bruker Kappa Apex II CCD (for **5** and **6**), a Bruker-Nonius X8 Apex CCD (for **7**) and a Bruker P4 (for **8**) diffractometer. Absorption corrections were applied by using the SADABS (for **5–7**) and XPREP (for **8**) programs. The structure was solved by direct methods implemented in the SHELXS-97 program^[26] and refined by the full-matrix least-squares method in an anisotropic approximation by using the SHELXL-97 program.^[26] The obtained crystal structures were analyzed for short contacts between nonbonded atoms with the PLATON program.^[20] CCDC-757826 (**5**), -757827 (**7**), -757828 (**6**) and -757829 (**8**) contain the supplementary crystallographic data for this paper; CCDC-604700 contains the data for compound **4**. These data can be obtained free of charge from The Cambridge Crystallographic Data Centre via www.ccdc.cam.ac.uk/data_request/cif. X-ray powder diffraction data for compound **8** were obtained with a DRON-3M automated diffractometer ($R = 192$ mm, Cu- K_{α} radiation, Ni-filter, scintillation point detector with amplitude discrimination, and 2.5° Soller slits on the primary and reflected beams) at room temperature over the 2θ range 3–50° with a step size of 0.02° in 2θ and 12 s counting time per step. An equatorial divergence slit of 2 mm and an axial divergence slit of 12 mm were used.

Quantum Chemical Calculations

DFT calculations were performed using the Gaussian 03 suite of programs^[27] applying standard gradient techniques at the B3LYP level of theory by using the 6-311+G* basis set on all atoms; the basis set was used as it is implemented in the program. Force-field calculations were used to ascertain whether the resulting structures were energy minima. The energies are not ZPE-corrected. All subsequent calculations of molecular properties were performed at the B3LYP/6-311+G* geometries. Chemical shielding factors were calculated at all atomic positions at the DFT/B3LYP/6-311+G* level of theory by using the GIAO method implemented in Gaussian 03. The chemical shift for the selenium atom was obtained by subtracting the chemical shielding value of this atom from that calculated for dimethylselenide, which is 1623.1500 ppm at the B3LYP/6-311+G* level of theory, based on the corresponding geometry (C_{2v} symmetry, *anti,anti*-conformer). Bond orders (or rather overlap populations; see ref. 15) were calculated according to the Hirshfeld scheme. QTAIM bond and ring properties were calculated by using the AIMPACK suite of programs.^[28]

Supporting Information (see footnote on the first page of this article): X-ray powder diffractogram of compound **8** (Figure S1), variable-temperature and variable-solvent ⁷⁷Se and ¹⁹F NMR spectra of compounds **4**, **7** and **8** (Figures S2–S6) and packing diagrams of compounds **4–8** (Figure S7) are available.

Table 9. Crystallographic and refinement data for compounds 5–8.

	5	6	7	8
Formula	C ₁₂ H ₈ Cl ₂ N ₂ S ₃	C ₁₂ H ₈ Cl ₂ N ₂ SSe ₂	C ₁₂ Cl ₂ F ₈ N ₂ S ₃	C ₁₂ Cl ₂ F ₈ N ₂ SSe ₂
<i>M</i>	347.28	441.08	491.25	585.03
<i>T</i> / K	150	173	150	203
λ / Å	0.71073	0.71073	0.71073	0.71073
Crystal system	monoclinic	orthorhombic	monoclinic	monoclinic
Space group	<i>P</i> 2 ₁	<i>P</i> 2 ₁ 2 ₁ 2 ₁	<i>P</i> 2 ₁ / <i>n</i>	<i>P</i> 2 ₁ / <i>c</i>
<i>a</i> / Å	3.8469(10)	3.9548(8)	6.0999(5)	13.519(5)
<i>b</i> / Å	11.510(3)	11.236(2)	29.3783(19)	14.592(8)
<i>c</i> / Å	15.785(4)	32.106(6)	9.1803(6)	8.567(3)
β / °	91.262(9)	90	96.391(2)	94.40(3)
<i>U</i> / Å ³	698.7(3)	1426.6(5)	1634.9(2)	1685.0(13)
<i>Z</i>	2	4	4	4
<i>D</i> _c / g cm ⁻³	1.651	2.054	1.996	2.306
μ / mm ⁻¹	0.897	5.689	0.866	4.913
<i>F</i> (000)	352	848	960	1104
Crystal size / mm	0.40 × 0.10 × 0.01	0.54 × 0.02 × 0.02	0.05 × 0.23 × 0.40	0.90 × 0.20 × 0.02
θ range / °	1.3–28.0	1.3–27.5	1.4–31.7	2.1–27.5
Index range	–4 ≤ <i>h</i> ≤ 5, –15 ≤ <i>k</i> ≤ 13, –20 ≤ <i>l</i> ≤ 20	–5 ≤ <i>h</i> ≤ 2, –14 ≤ <i>k</i> ≤ 14, –41 ≤ <i>l</i> ≤ 40	–8 ≤ <i>h</i> ≤ 8, –25 ≤ <i>k</i> ≤ 43, –11 ≤ <i>l</i> ≤ 13	–17 ≤ <i>h</i> ≤ 17, 0 ≤ <i>k</i> ≤ 18, –11 ≤ <i>l</i> ≤ 0
Reflections collected	5561	9044	15273	3946
Independent reflections	3081, [<i>R</i> _{int} = 0.0600]	3218, [<i>R</i> _{int} = 0.0983]	5445, [<i>R</i> _{int} = 0.0524]	3782, [<i>R</i> _{int} = 0.0393]
Completeness to θ / %	99.1	99.9	98.7	97.9
Absorption correction	Empirical	Empirical	Empirical	Integration
Refinement method	Full-matrix least-squares on <i>F</i> ²	Full-matrix least-squares on <i>F</i> ²	Full-matrix least-squares on <i>F</i> ²	Full-matrix least-squares on <i>F</i> ²
Data, restraints, parameters	3081, 1, 173	3218, 0, 173	5445, 0, 244	3782, 0, 244
Goodness-of-fit on <i>F</i> ²	1.081	1.021	1.110	1.015
Observed reflections	2391	2623	4786	2280
Final <i>R</i> indices [<i>I</i> > 2 σ (<i>I</i>)]	<i>R</i> ₁ = 0.0424	<i>R</i> ₁ = 0.0647	<i>R</i> ₁ = 0.0468	<i>R</i> ₁ = 0.0748
<i>R</i> indices (all data)	<i>wR</i> ₂ = 0.0971	<i>wR</i> ₂ = 0.1021	<i>wR</i> ₂ = 0.1142	<i>wR</i> ₂ = 0.2183
Largest diff. peak and hole (e / Å ⁻³)	0.56; –0.58	0.69; –1.40	0.70; –0.75	0.76; –0.77

Acknowledgments

The authors are grateful to the Russian Foundation for Basic Research (project no. 09–03–00361) and the University of Antwerp (project BOF UA 22296) for financial support. The authors also gratefully acknowledge the University of Antwerp for access to the university's computer cluster CalcUA.

- [1] a) A. J. Banister, I. B. Gorrell, *Adv. Mater.* **1998**, *10*, 1415–1429; b) M. M. Labes, P. Love, L. F. Nichols, *Chem. Rev.* **1979**, *79*, 1–15.
- [2] a) R. C. Mawhinney, J. D. Goddard, *THEOCHEM* **2008**, *856*, 16–29; b) A. Modelli, N. Ventura, F. Scagnolari, M. Contento, D. Jones, *J. Phys. Chem. A* **2001**, *105*, 219–226; c) J. M. Rawson, J. J. Longridge, *Chem. Soc. Rev.* **1997**, *26*, 53–61; d) A. V. Zibarev, A. O. Miller, Yu. V. Gatilov, G. G. Furin, *Heteroat. Chem.* **1990**, *1*, 443–453.
- [3] a) H. M. Tuononen, R. J. Suontamo, J. U. Valkonen, R. S. Laitinen, T. Chivers, *Inorg. Chem.* **2003**, *42*, 2447–2454; b) M. Zahedi, S. Shahbazian, S. Weng Ng, *THEOCHEM* **2003**, *629*, 91–104; c) N. Sandblom, T. Ziegler, T. Chivers, *Inorg. Chem.* **1998**, *37*, 354–359.
- [4] T. Maaninen, H. M. Tuononen, K. Kosunen, R. Oilunkaniemi, J. Hiitola, R. S. Laitinen, T. Chivers, *Z. Anorg. Allg. Chem.* **2004**, *630*, 1947–1954.
- [5] a) E. Lork, R. Mews, M. M. Shkirov, P. G. Watson, A. V. Zibarev, *Eur. J. Inorg. Chem.* **2001**, 2123–2134; b) I. Yu. Bagryanskaya, Yu. V. Gatilov, A. V. Zibarev, *Mendeleev Commun.* **1999**, 157–158; c) I. Yu. Bagryanskaya, Yu. V. Gatilov, A. V. Zibarev, *Zh. Strukt. Khim.* **1999**, *40*, 790–793 (in Russian); d) I. Yu. Bagryanskaya, Yu. V. Gatilov, M. M. Shkirov, A. V. Zibarev, *Mendeleev Commun.* **1994**, 167–169; e) I. Yu. Bagryanskaya, Yu. V. Gatilov, M. M. Shkirov, A. V. Zibarev, *Mendeleev Commun.* **1994**, 136–137; f) V. Busetti, G. Cevasco, G. Leandri, Z. *Krystallogr.* **1991**, *197*, 41–50; g) V. Busetti, *Acta Crystallogr., Sect. B* **1982**, *38*, 665–667; h) G. Leandri, V. Busetti, G. Valle, M. Mammì, *J. Chem. Soc. C* **1970**, 413–414.
- [6] a) I. Yu. Bagryanskaya, Yu. V. Gatilov, M. M. Shkirov, A. V. Zibarev, *J. Struct. Chem.* **1996**, *37*, 318–322; b) K. Bestari, R. T. Oakley, A. W. Cordes, *Can. J. Chem.* **1991**, *69*, 94–99.
- [7] a) K. Tersago, I. Yu. Bagryanskaya, Yu. V. Gatilov, S. A. Gromilov, A. Yu. Makarov, M. Mandado, C. Van Alsenoy, A. V. Zibarev, F. Blockhuys, *Eur. J. Inorg. Chem.* **2007**, 1958–1965; b) K. Tersago, M. Mandado, C. Van Alsenoy, I. Yu. Bagryanskaya, M. K. Kovalev, A. Yu. Makarov, Yu. V. Gatilov, M. M. Shkirov, A. V. Zibarev, F. Blockhuys, *Chem. Eur. J.* **2005**, *11*, 4544–4551; c) F. P. Olsen, J. C. Barrick, *Inorg. Chem.* **1973**, *12*, 1353–1355; d) J. Leitch, S. C. Nyburg, D. A. Armitage, M. J. Clark, *J. Cryst. Mol. Struct.* **1973**, *3*, 337–332.
- [8] A. V. Zibarev, A. O. Miller, Yu. V. Gatilov, G. G. Furin, *Heteroat. Chem.* **1990**, *1*, 443–453.
- [9] G. Wolmershaeuser, P. R. Mann, *Z. Naturforsch., Teil B* **1991**, *46*, 315–319.
- [10] Yu. V. Zefirov, *Krystallografiya* **1997**, *42*, 936–958 (in Russian).
- [11] a) A. F. Cozzolino, J. F. Britten, I. Vargas-Baca, *Cryst. Growth Des.* **2006**, *6*, 181–186; b) A. F. Cozzolino, I. Vargas-Baca, S. Mansour, A. H. Mahmoudkhani, *J. Am. Chem. Soc.* **2005**, *127*, 3184–3190; c) A. J. Zhou, S. L. Zheng, M. L. Tong, *Inorg. Chem.* **2005**, *44*, 4457–4459.
- [12] a) R. S. Rowland, R. Taylor, *J. Phys. Chem.* **1996**, *100*, 7384–7391; b) A. Bondi, *J. Phys. Chem.* **1964**, *68*, 441–451.
- [13] K. Kuchitsu, S. J. Cyvin in *Molecular Structures and Vibrations* (Ed.: S. J. Cyvin), Elsevier, Amsterdam, **1972**.

- [14] E. A. V. Ebsworth, D. W. H. Rankin, S. Craddock, *Structural Methods in Inorganic Chemistry*, Blackwell, Oxford, **1991**.
- [15] J. Oláh, F. Blockhuys, T. Veszprémi, C. Van Alsenoy, *Eur. J. Inorg. Chem.* **2006**, 69–77.
- [16] R. F. W. Bader, *Atoms in Molecules: A Quantum Theory*, Oxford University Press, Oxford, **1990**.
- [17] a) W. Sicinska, L. Stefaniak, M. Witanowski, G. A. Webb, *J. Mol. Struct.* **1987**, 158, 57–68; b) J. Kuyper, K. Vrieze, *J. Organomet. Chem.* **1975**, 86, 127–138.
- [18] a) A. V. Zibarev, M. A. Fedotov, G. G. Furin, *Izv. Akad. Nauk SSSR, Ser. Khim.* **1989**, 829–832 (in Russian; *Chem. Abstr.* **111**, 173485); b) G. G. Furin, A. I. Rezvukhin, M. A. Fedotov, G. G. Yakobson, *J. Fluorine Chem.* **1983**, 22, 231–252.
- [19] A. Gavezzotti, *OPiX, A Computer Program Package for the Calculation of Intermolecular Interactions and Crystal Energies*, May **2006** version, Dipartimento di Chimica Structurale e Stereochimica Inorganica, Università di Milano, Milano, Italy.
- [20] a) A. L. Spek, *PLATON, A Multipurpose Crystallographic Tool*, Version 10M, Utrecht University, Utrecht, The Netherlands, **2003**; b) A. L. Spek, *J. Appl. Crystallogr.* **2003**, 36, 7–17.
- [21] *Cambridge Structural Database*, Version 5.31 (updates February **2010**), filters and restrictions were not applied.
- [22] I. Yu. Bagryanskaya, Yu. V. Gatilov, A. O. Miller, M. M. Shakirov, A. V. Zibarev, *Heteroat. Chem.* **1994**, 5, 561–565.
- [23] a) K. Pilgram, D. D. Philips, *J. Org. Chem.* **1965**, 30, 2388–2392; b) O. Behaghel, H. Seibert, *Ber. Dtsch. Chem. Ges.* **1933**, 66, 708–716.
- [24] a) J. Burdon, D. R. King, J. C. Tatlow, *Tetrahedron* **1966**, 22, 2541–2549; b) G. G. Yakobson, V. D. Shteingarts, N. E. Mironova, N. N. Vorozhtsov, *J. Gen. Chem. USSR* **1966**, 36, 150–152.
- [25] A. Yu. Makarov, I. Yu. Bagryanskaya, F. Blockhuys, C. Van Alsenoy, Yu. V. Gatilov, V. V. Knyazev, A. M. Maksimov, T. V. Mikhailina, V. E. Platonov, M. M. Shakirov, A. V. Zibarev, *Eur. J. Inorg. Chem.* **2003**, 77–88.
- [26] G. M. Sheldrick, *SHELX-97 – Programs for Crystal Structure Analysis*, Release 97–2, University of Göttingen, Göttingen, Germany.
- [27] M. J. Frisch, G. W. Trucks, H. B. Schlegel, G. E. Scuseria, M. A. Robb, J. R. Cheeseman, J. A. Montgomery Jr., T. Vreven, K. N. Kudin, J. C. Burant, J. M. Millam, S. S. Iyengar, J. Tomasi, V. Barone, B. Mennucci, M. Cossi, G. Scalmani, N. Rega, G. A. Petersson, H. Nakatsuji, M. Hada, M. Ehara, K. Toyota, R. Fukuda, J. Hasegawa, M. Ishida, T. Nakajima, Y. Honda, O. Kitao, H. Nakai, M. Klene, X. Li, J. E. Knox, H. P. Hratchian, J. B. Cross, C. Adamo, J. Jaramillo, R. Gomperts, R. E. Stratmann, O. Yazyev, A. J. Austin, R. Cammi, C. Pomelli, J. W. Ochterski, P. Y. Ayala, K. Morokuma, G. A. Voth, P. Salvador, J. J. Dannenberg, V. G. Zakrzewski, S. Dapprich, A. D. Daniels, M. C. Strain, O. Farkas, D. K. Malick, A. D. Rabuck, K. Raghavachari, J. B. Foresman, J. V. Ortiz, Q. Cui, A. G. Baboul, S. Clifford, J. Cioslowski, B. B. Stefanov, G. Liu, A. Liashenko, P. Piskorz, I. Komaromi, R. L. Martin, D. J. Fox, T. Keith, M. A. Al-Laham, C. Y. Peng, A. Nanayakkara, M. Challacombe, P. M. W. Gill, B. Johnson, W. Chen, M. W. Wong, C. Gonzalez, J. A. Pople, *Gaussian 03, Revision C.02*, Gaussian, Inc., Wallingford CT, **2004**.
- [28] R. F. W. Bader et al., *AIMPAC: A Suite of Programs for the AIM Theory*, McMaster University, Hamilton, Ontario, Canada.

Received: May 31, 2010
Published Online: August 24, 2010